Implication of the Autologous Immune System in BCR-ABL Transcript Variations in Chronic Myelogenous Leukemia Patients Treated with Imatinib.

Geoffrey D Clapp, Thomas Lepoutre, Raouf El Cheikh, Samuel Bernard, Jérémy Ruby, Hélène Labussière-Wallet, Franck E Nicolini, Doron Levy

▶ **To cite this version:**

Geoffrey D Clapp, Thomas Lepoutre, Raouf El Cheikh, Samuel Bernard, Jérémy Ruby, et al.. Implication of the Autologous Immune System in BCR-ABL Transcript Variations in Chronic Myelogenous Leukemia Patients Treated with Imatinib.. Cancer Research, 2015, 75 (19), pp.4053-62. 10.1158/0008-5472.CAN-15-0611 . hal-01251396

HAL Id: hal-01251396
https://inria.hal.science/hal-01251396

Submitted on 18 Jan 2017

HAL is a multi-disciplinary open access archive for the deposit and dissemination of scientific research documents, whether they are published or not. The documents may come from teaching and research institutions in France or abroad, or from public or private research centers.

L'archive ouverte pluridisciplinaire **HAL**, est destinée au dépôt et à la diffusion de documents scientifiques de niveau recherche, publiés ou non, émanant des établissements d'enseignement et de recherche français ou étrangers, des laboratoires publics ou privés.

BCR-ABL transcripts variations in chronic phase chronic myelogenous leukemia patients on imatinib: Possible role of the autologous immune system

Authors: Geoffrey D. Clapp[1], Thomas Lepoutre[2], Raouf El Cheikh[2], Samuel Bernard[2], Jérémy Ruby[3], Hélène Labussière-Wallet[3], Franck E. Nicolini[3], Doron Levy[4]

Affiliations:

1 Department of Mathematics, University of Maryland, College Park, MD 20742, USA

2 Inria, and Université de Lyon, Université Claude Bernard Lyon 1, CNRS UMR 5208, Institut Camille Jordan, 43 blvd. du 11 novembre 1918, F-69622 Villeurbanne cedex, France

3 Centre Hospitalier Lyon, Sud, Pierre-Bénite France and CRCL, Centre Léon Bérard, Lyon, France,

4 Department of Mathematics and Center for Scientific Computation and Mathematical Modeling (CSCAMM), University of Maryland, College Park, MD 20742, USA

Corresponding author: Doron Levy

Department of Mathematics and Center for Scientific Computation and Mathematical Modeling (CSCAMM), University of Maryland, College Park, MD 20742, USA

Email: dlevy@math.umd.edu

Phone: (301)405-5140

Fax: (301)-314-6674

Key words: CML, BCR-ABL, TKI, immune system

Short title: Autologous immune system and chronic phase CML

Abstract

Tyrosine kinase inhibitors (TKIs), such as imatinib (IM), have significantly improved treatment of chronic myelogenous leukemia (CML). However, the majority of patients are not cured for undetermined reasons. A more complete understanding of their mechanisms of action would help to identify limitations of TKI therapy alone and could inform the use of combination therapies aimed at controlling or definitively eradicating the residual leukemic population. Based on our patients' data, we found that many patients who otherwise responded well to IM therapy still showed variations in their BCR-ABL transcripts. To investigate this phenomenon, we applied a mathematical model that integrates CML and an autologous immune response to the patients' data. We define an immune window, or a range of leukemic loads for which the autologous immune system induces an improved response. Our modeling results suggest that, at diagnosis, a patient's leukemic load is able to partially or fully suppress the autologous immune response developed in a majority of patients, towards the CML clone(s). IM therapy drives the leukemic population into the "immune window", allowing the patient's autologous immune cells to expand and eventually mount an efficient recognition of the residual leukemic burden. This response drives the leukemic load below this immune window, allowing the leukemic population to partially recover until another weaker immune response is initiated. Thus, the autologous immune response may explain the oscillations in the BCR-ABL transcripts regularly observed in patients on IM.

Major Findings:

Based on patient data and our model, we hypothesize that the autologous immune system plays a significant role in the dynamics of CML during IM therapy. Moreover, variations in the BCR-

ABL transcripts during IM therapy may represent a signature of the patient's individual autologous immune response. Immunotherapy may complement IM and other TKIs by helping to maintain a patient's autologous immune response when the leukemia stimulus alone is insufficient. Our mathematical model is a potentially valuable tool in studying and designing patient-specific schedules for these combination therapies.

Introduction

Chronic myeloid leukemia (CML) is a myeloproliferative disorder caused by the BCR-ABL fusion oncogene, which encodes for a constitutively active tyrosine kinase. Tyrosine kinase inhibitors (TKI), such as imatinib (IM), are targeted therapies that have revolutionized the treatment of CML, producing durable remissions in many patients and resulting in substantially improved long-term survival rates [1, 2]. Despite their success, their global therapeutic effect remains incompletely understood. Moreover, it is unclear whether TKIs alone are capable of eliminating the entire leukemic burden, as many patients in long-term remissions continue to harbor small residual leukemic loads even after many years of therapy [3]. A better understanding of TKIs would allow us to improve the way that these drugs are administered and also to identify their limitations. If TKIs prove to be incapable of curing most patients, then understanding the drugs' mechanisms of action may inform our use of combination therapies.

There is compelling evidence that a patient's autologous immune response plays a significant role in the dynamics of CML. It is known that immune cells are capable of detecting and eliminating cancer cells [4]. Immunotherapy is a major goal of immunology and cancer research because of the ability of the immune system to target and eliminate abnormal cells while leaving healthy cells intact. In the allogeneic setting, the immune system has demonstrated its power in the elimination of residual CML disease [5]. Several combination therapies involving interferon-alfa (IFN-α) are currently being investigated [6, 7, 8], in part, because of this drug's effects on the autologous immune system [8], which participates in the control of the disease. Additionally, IFN-α may drive quiescent leukemic stem cells into the cell cycle [9, 10], where they become exposed to the effects of TKIs.

In the Stop Imatinib (STIM) [11] and TWISTER [3] trials, patients who responded well to IM were taken off therapy in order to determine whether treatment-free remission (TFR) could be achieved. They found that approximately 40% of patients remained in TFR for at least two years after stopping treatment. Moreover, although not statistically significant, the TFR rate was higher in patients that had received interferon prior to IM [11]. In many of these patients, BCR-ABL DNA and mRNA were still detectable [3]. Moreover, in [12], patients still harbored BCR-ABL+ leukemic stem cells, despite having remained in TFR for up to eight years. In these cases, since treatment did not completely eradicate the disease, some other mechanisms, such as the autologous immune system, must be preventing this residual cancer population from expanding. Motivated by these results, we constructed a mathematical model integrating CML and the autologous immune response.

Materials and Methods

A group of 104 patients with CML was monitored during IM therapy in the Centre Hospitalier Lyon Sud. These patients were all treated with first-line IM 400 mg daily. Patients' BCR-ABL ratios were measured in the same laboratory, with the same technique at diagnosis, at months 3, 6, 9, and 12 of therapy, and every 6 months thereafter. Overall, the patients had an average follow-up time of 62.76 months (range: 2.96 - 148.70), with an average of 12.69 measurements taken (range: 2 - 26). We excluded patients who changed TKIs for safety reasons (n = 33) and patients whose disease progressed (n = 14), as we focused exclusively in this study on patients obtaining a residual disease on IM. Thus, a population of 65 patients who responded well to IM remained for analysis.

BCR-ABL ratios were serially measured by quantitative RT-PCR in the peripheral blood of patients in a single laboratory according to the European standards of European Leukemia Net [13, 14]. Each sampling was run in parallel to the previous (frozen) sample from each patient in order to exclude technical problems, at each time point (except diagnosis) for all patients.

Our mathematical model divides leukemic cells into quiescent stem cells (y_0), cycling stem cells (y_1), progenitors (y_2), and mature cells (y_3). We also represent a single autologous immune cell population (z). For simplicity, we do not distinguish further between immune subpopulations. Leukemia cells stimulate immune cells to proliferate at a maximum rate α, while immune cells kill leukemia cells at a maximum rate μ. We incorporate immunosuppression by inhibiting the proliferation of the immune cells as well as their action on leukemic cells. Our model is summarized in Figure 1. A more thorough description of the model is provided in the "Quick Guide to Equations and Assumptions."

The BCR-ABL ratio is a blood measurement that quantifies the amount of BCR-ABL transcript relative to a control transcript, BCR or ABL (here, ABL). Each leukemic cell possesses the BCR-ABL gene and the normal allele of ABL gene, while healthy cells (x) possess two alleles of the ABL gene. Therefore, BCR-ABL transcripts are proportional to y_3 (the immature leukemia cell populations are much smaller than the mature population and can be neglected), while control transcripts are approximately proportional to $2x + y_3$. For simplicity, the number of healthy cells (x) is assumed to be constant and is estimated based on the patient's initial BCR-ABL ratio at diagnosis. For all later measurements, the BCR-ABL ratio is approximated by

$$\text{ratio} \approx 100\beta \frac{y_3}{2x + y_3}$$

The multiplication factor β accounts for differences in mRNA expression between BCR-ABL and the control gene. We multiply by 100, in order to convert the ratio into a percentage when β = 1 and a value between 0 and 100β otherwise.

Quick Guide to Equations and Assumptions

We develop an ODE model of CML and the immune system, to study the dynamics of IM therapy. Specifically, we seek to understand patients whose BCR-ABL ratios vary non-monotonically during therapy.

Let y_0, y_1, and y_2, and y_3 represent the concentrations of quiescent leukemic stem cells, cycling leukemic stem cells, progenitor leukemic cells, and mature leukemic cells. Let z denote the concentration of immune cells. We consider the following system of ODEs.

$$\dot{y}_0 = b_1 y_1 - a_0 y_0 - \frac{\mu y_0 z}{1 + \varepsilon y_3^2} \tag{1}$$

$$\dot{y}_1 = a_0 y_0 - b_1 y_1 + r y_1 \left(1 - \frac{y_1}{K}\right) - d_1 y_1 - \frac{\mu y_1 z}{1 + \varepsilon y_3^2} \tag{2}$$

$$\dot{y}_2 = a_1 y_1 - d_2 y_2 - \frac{\mu y_2 z}{1 + \varepsilon y_3^2} \tag{3}$$

$$\dot{y}_3 = a_2 y_2 - d_3 y_3 - \frac{\mu y_3 z}{1 + \varepsilon y_3^2} \tag{4}$$

$$\dot{z} = s_z - d_z z + \frac{\alpha y_3 z}{1 + \varepsilon y_3^2} \tag{5}$$

In Equations (1) and (2), a_0 and b_1 represent the transition rates of leukemic stem cells from quiescence to cycling and cycling to quiescence, respectively. We assume logistic growth of cycling stem cells, with growth rate r and carrying capacity K. Cycling stem cells die naturally at a rate d_1. In Equation (3), the first term represents the differentiation of stem cells into progenitors. The coefficient a_1 is the product of the differentiation rate and the amplification factor upon differentiation due to cell proliferation. Progenitors die naturally at a rate d_2. Equation (4) is similar to (3), with differentiation rate a_2 and death rate d_3. The last terms in

Equations (1)-(4) represent the death of leukemic cells caused by an immune response. The mass action term $\mu y_i z$ represents the killing of leukemic cells by the immune system, where μ is the maximal rate (per immune cell) at which an immune cell will engage and kill a leukemic cell. Equation (5) represents the concentration of autologous immune cells. The first term, s_z, is a constant source term. Immune cells die at a rate d_z. The mass action term $\alpha y_3 z$ represents the expansion (proliferation) of the immune cell pool in response to its leukemia stimulus, which occurs with maximal rate per leukemic cell α. We include only the contributions of the mature leukemic cells y_3 to immune stimulation since they are a much larger population than the immature leukemic cells ($y_{total} \approx y_3$).

Our model is based on the assumption that immunosuppression acts in two ways. First, mature leukemic cells inhibit the expansion of immune cells. In Equation 5, the immune cell expansion term $\alpha y_3 z$ is divided by $1 + \varepsilon y_3^2$, where the constant ε determines the strength of the immunosuppression. Second, mature leukemic cells are assumed to decrease the killing capacity μ of activated immune cells, also by a factor of $1 + \varepsilon y_3^2$. This effect is represented in the last terms in Equations (1)-(4). This approach is similar to the one used in [15]. By implementing immunosuppression in this way, we encode an autologous immune response that is effective only with intermediate levels of leukemic cells. When the leukemic load is small, only a small number of immune cells is stimulated to respond. On the other hand, although large leukemic loads provide a stronger stimulus, the leukemic cells are able to suppress the efficacy of the immune system. Thus, the immune response will be negligible when the leukemic load is either very small, at levels undetectable by the immune system, or very large, at levels that overwhelm and suppress the immune system. A strong immune response can occur only when the leukemic load y_3 is at an intermediate level, within a range $[y_{min}, y_{max}]$ that we call the immune window. In our

model, we define the immune window as the range of y_3 for which the rate of immune stimulation ($\frac{\alpha y_3}{1+\varepsilon y_3^2}$) exceeds the death rate (d_z). IM therapy may be used to drive the leukemic load into this immune window, allowing the autologous immune system to assist the drug in the elimination of the leukemic cells.

IM is known to block the kinase activity of the BCR-ABL protein, which results in a significant decrease in the proliferation rates of the BCR-ABL$^+$ leukemic cells [1, 16] and apoptotic death [17]. However, we focus here on the effects of IM on proliferation and leave incorporation of other mechanisms to a future work. We implement IM therapy in the model by decreasing the differentiation/amplification rates a_1 and a_2 to lower values $a_1' = a_1 / inh_1$ and $a_2' = a_2 / inh_2$. It is unknown how IM affect LSCs and whether quiescent LSCs are affected at all, so we assume no direct effect of IM on these populations. However, our model provides a framework for testing various mechanisms of actions of IM, which we leave for a future work.

It is also unclear whether IM is capable of completely eliminating the leukemic cell burden, or whether small residual populations will persist indefinitely. In our model, a leukemic load of zero can only be approached asymptotically, so we define cure as a cancer stem cell concentration less than $1.67(10)^{-4}$ cells/mL, which corresponds to less than one leukemic stem cell. We stop all simulations of the model whenever this is achieved.

Results

Many patients who otherwise respond well to therapy exhibit oscillations in their BCR-ABL ratios. Of the 104 patients in our data set, only 15 showed monotonically decreasing BCR-ABL ratios throughout therapy. Each of the remaining 89 patients showed increases in BCR-ABL ratios in, on average, 28.82% of their measurements. Two representative patients are shown in Figure 2. These fluctuations occurred in many patients who responded well to IM therapy and did not have any adverse events. This lack of monotonicity in patients who responded well to therapy motivated this study.

We applied our mathematical model, which is summarized in Figure 1, to the patient data in order to study these oscillations. As previously mentioned, our model represents leukemic cells of varying maturity and a single immune cell population. We applied Latin hypercube sampling in order to determine the effect of the drug (a_1' and a_2') and the immune parameters (μ, d_z, α, and ε). The parameters d_z, α, and ε determine the patient's immune window $[y_{min}, y_{max}]$, or the range of leukemia loads that will stimulate a strong immune response. We define $[y_{min}, y_{max}]$ by the range of y_3 for which the level of immune stimulation exceeds the death rate. For each patient, we selected the parameter set that minimizes the squared log-distance between the patient data and the results of the model simulation (sampled at the same time as the data). All other parameters were held constant across all patients; their values can be found in Table S1 of the Supplementary Material. The patient-specific parameter values are summarized in Table 1. Figures 3 and 4 show representative fits of our model to patient data. (The patient-specific parameters producing these fits are provided in Table S2 of the Supplementary Material.)

Keeping in mind that these fits are plotted on a logarithmic scale, we see that our model is able to reproduce many patients' dynamics during therapy.

The patient data and modeling results suggest that patients who respond well to IM therapy go through three to four phases of tumor reduction. During the first few months, there is a rapid exponential decline in BCR-ABL ratio. In our model, this effect is due primarily to the action of the drug on the mature leukemic population. The immune response is negligible at this stage because the large leukemic load suppresses the immune system. Beginning around month six, there is a second, slower exponential decline in BCR-ABL ratio. In some patients, the second phase is a plateau in BCR-ABL ratio rather than a decline (see Figures 3d). The location of this plateau is determined primarily by the direct effects of IM on the leukemic cell population (parameters inh_1 and inh_2). This biphasic exponential decline has been previously observed in [18] and [19]. A few patients show a triphasic exponential decline (Figures 4b-d), which was discussed in [20].

The duration of the biphasic or triphasic decline can vary significantly between patients, from the first two years (Figures 3a, 3c, 3d, 4f) to several years of therapy (Figures 4b-d). After this period of monotonic decline, many patients' leukemic loads begin to vary non-monotonically. In our model, these variations are explained by an autologous immune response that occurs after therapy drives the leukemic population into the immune window. When the leukemic population enters the immune window, the immune cells continue to expand until they can mount a first attack on the leukemic cells. This first attack results in a sharp decline in the leukemic population, as in Figures 3f, 4b, and 4d-f, and often produces the minimum leukemic burden achieved during therapy. If this first response is sufficiently strong, it may drive the leukemic stem cell population to less than one cell, which we interpret as cure in our model.

Otherwise, the immune cells contract once the leukemic population falls below the immune window, and the leukemic population is able to partially recover. Several oscillations between the leukemic and immune cells follow, with their amplitudes decreasing over time as the populations approach an equilibrium, as seen in Figure 5.

The patient-specific parameters are summarized in Table 1. Of the six parameters varied, the fits seem to be most sensitive to inh_1 and inh_2, followed by y_{min} and y_{max}. The parameters d_z and μ seem to be less important. This is not surprising, as inh_1 and inh_2 determine the effect of the drug, and y_{min} and y_{max} determine at what point the autologous immune response becomes significant. Scatter plots depicting parameter sensitivities for a representative patient are shown in Figure 6.

The parameter values in Table 1 suggest that IM alone results in a 3.5-log decrease in the total leukemia load, on average (STD: 0.786, max: 5.158, min: 2.426). This effect is divided into a 2.5-log decrease in the proliferation of mature cells and a 1-log decrease in the proliferation of progenitors. Each patient's immune window covers approximately one order of magnitude of leukemic populations, generally falling between $10^{2.5}$ cells/mL and 10^6 cells/mL. We assume an initial mature leukemic population of $1.5(10)^8$ cells/mL. Thus, IM must decrease the leukemia load by several orders of magnitude before the leukemia enters the immune window and an immune response is initiated. After the leukemic population enters this window, the leukemia and immune populations oscillate, with the amplitude of oscillations decreasing over time.

Discussion

Despite the success of IM and other TKI therapies, many questions about the underlying mechanisms of action remain. Mathematical modeling is a complementary tool to clinical and experimental data that can help us understand these mechanisms. Several mathematical modeling groups have already studied various aspects of CML [15, 18, 19, 21, 22, 23, 24]. We briefly review some of these contributions but note that a more thorough review can be found in [25].

Michor et al. [18] constructed an ordinary differential equations (ODE) model of CML that divides leukemic cells into stem cells, progenitors, differentiated cells, and terminally differentiated cells. Upon analyzing patients' initial responses to IM therapy, they found that IM often lead to biphasic exponential declines in the leukemic cell populations. Their modeling results suggested that the first, steeper decline represents the action of IM on the differentiated leukemic cell population, while the second, slower decline represents an effect on the leukemic progenitors. They later hypothesized that long-term therapy leads to a triphasic exponential decline, where the third decline may represent an effect on immature leukemic cells and possibly leukemic stem cells [20].

On the other hand, Roeder et al. [19] developed an agent-based model of CML that divides leukemic stem cells into cycling and quiescent compartments. In their model, IM results in the degradation and inhibition of cycling leukemic stem cells while having no direct effect on quiescent leukemic stem cells. They interpreted the biphasic exponential decline as an initial degradation effect, followed by a change in the regulatory response of leukemic stem cells which produces the second decline. A similar interpretation to the biphasic decline is proposed in [22].

Although these modeling frameworks are capable of reproducing the dynamics of some patients during therapy, both are limited to those who show a monotonic decline in their

leukemic burdens. Neither model includes a mechanism that would allow patients to show oscillations in leukemia load. However, in our data, we found that many patients who respond well to IM and achieve long-term remissions exhibit increases in leukemic burden. The fact that the Michor and Roeder models are unable to reproduce such oscillations suggests that there may be (an) additional mechanism(s) that contribute(s) to patients' dynamics during therapy.

Motivated by this, we developed a mathematical model that integrates CML and an autologous immune response. As previously mentioned, there is strong evidence that the immune system plays a role in the dynamics of CML [3, 4, 8, 26, 27]. In our modeling framework, we defined an immune window, or a range of leukemic loads that will provoke a strong autologous immune response. At diagnosis, the leukemic load is above this window, and the large leukemic population is able to partially or fully suppress the autologous immune system's response to CML. IM therapy generally reduces a patient's leukemic load by several orders of magnitude, representing a significant reduction in immunosuppression. We hypothesize that IM may drive the leukemic population into the immune window, allowing a patient's autologous immune system to mount a response to CML.

In our model, oscillations in leukemic load occur after the leukemia enters the immune window. Once the autologous immune cells have expanded sufficiently, they attack the residual leukemic population. This first attack by the autologous immune system results in the minimum detectable leukemic load achieved during IM therapy. However, because the leukemia is driven below the immune window, the patient's immune cells begin to contract. If the leukemia is not eradicated, it is able to rebound, until it reenters the immune window, thus stimulating another weaker immune response. The immune and leukemic cell populations continue to oscillate in this way, with the amplitude of these oscillations decreasing over time. Eventually, the oscillations

dampen, and an equilibrium is achieved between the leukemic and autologous immune cells.

Our modeling results suggest that oscillations in BCR-ABL ratio during therapy may be partially explained by the patient's autologous immune response to the residual CML population. Moreover, the oscillations may be a signature of the autologous immune response, that can be used to characterize a patient's individual immune system. Each patient's immune profile is different, as demonstrated by differences in the immune windows and in the timing and magnitude of the autologous immune response to CML. Our modeling framework provides a potential tool to help quantify these differences, which may play a significant role in designing personalized therapies or combination therapies aimed at eradicating the residual CML burden.

Conclusion

The potentially significant role of the immune system in the dynamics of IM therapy suggests that immunotherapy may help to eliminate the residual leukemic burden. In our simulations, when IM therapy drives the leukemia into the immune window, an initially strong immune response occurs that weakens over time. Eventually, the immune cell population contracts, allowing the leukemia to partially recover. A combination of IM and immunotherapy may help to maintain a strong immune response, to prevent such a recovery in the leukemic population. As suggested in [15], carefully-timed vaccines may stimulate the patient's immune system when the residual CML burden is no longer sufficient. A sustained immune response may result in a further decrease of the leukemic population and may even drive the leukemia to extinction. An optimal vaccine schedule would depend heavily on each patient's immune profile, and our model offers a tool for characterizing this.

Although we focus on the autologous immune response as a possible explanation of the oscillations that occur during IM therapy, many other factors may contribute to this behavior. The microenvironment of the leukemic cells is known to have a strong influence on both healthy and leukemic cells [28, 29], but is not included in our model. Additionally, we do not account for patients who do not properly or regularly take their drugs, which is known to be an important factor [30]. Moreover, for simplicity, we do not distinguish between various subtypes of immune cells, each of which may interact and play different roles in CML. Our model can be expanded in order to achieve a more accurate representation of the autologous immune response to CML. We leave this for a future work.

Still, the oscillations in patients' leukemic loads suggest an additional mechanism during therapy that has not previously been included in mathematical models. Our modeling results

support the hypothesis that the autologous immune system contributes to the dynamics of IM therapy. If this is the case, our model may serve as a valuable tool for characterizing a patient's immune response to CML. This immune profile may then help in designing personalized combination therapies in order to eliminate or control the residual leukemic burden.

ACKNOWLEDGEMENTS

The work of GC was supported by the National Science Foundation Graduate Research Fellowship under Grant No. DGE1322106. The work of DL was supported in part by the John Simon Guggenheim Memorial Foundation and by the National Science Foundation under Grant No. DMS-0758374. Any opinions, findings, and conclusions or recommendations expressed in this material are those of the authors and do not necessarily reflect the views of the National Science Foundation. FN thanks all the members of the clinical and routine laboratory teams for the valuable and continuous work for the care of our patients, the association "Regarde un jour le monde" for its support and patients themselves for participating in this study.

DISCLOSURES

Dr. F. Nicolini is a consultant for Novartis, Teva and Bristol Myers Squibb, benefits from a research grant from Novartis and is a member of the speakers bureau of Novartis, BMS and Ariad. The other authors have nothing to disclose. Dr. H. Labussière-Wallet has been a board member for Bristol Myers Squibb.

Bibliography

1. An X, Tiwari AK, Sun Y, Ding P-R, Ashby Jr CR, and Z-S Chen. BCR-ABL tyrosine kinase inhibitors in the treatment of Philadelphia chromosome positive chronic myeloid leukemia: A review Leukemia Research 2010;34:1255-68.

2. O'Brien SG, Guilhot F, Larson RA, Gathmann I, Baccarani M, Cervantes F, et al. Imatinib compared with interferon and low-dose cytarabine for newly diagnosed chronic-phase chronic myeloid leukemia. N Engl J Med 2003;348(11):994-1004.

3. Ross DM, Branford S, Seymour JF, Schwarer AP, Arthur C, Yeung DT, et al. Safety and efficacy of imatinib cessation for CML patients with stable undetectable minimal residual disease: results from the TWISTER study. Blood 2013;122:515-22.

4. Murphy K and P Travers. Janeway's Immunobiology 8th ed. New York: Garland Science, 2012 Print

5. Kolb HJ, Schattenberg A, Goldman JM, Hertenstein B, Jacobsen N, Arcese W, et al. Graft-versus-leukemia effect of donor lymphocyte transfusions in marrow grafted patients European Group for Blood and Marrow Transplantation Working Party Chronic Leukemia. Blood 1995;86(5):2041-50.

6. Hehlmann R, Lauseker M, Jung-Munkwitz S, Leitner A, Müller MC, Pletsch N, et al. Tolerability-adapted imatinib 800 mg/d versus 400 mg/d versus 400 mg/d plus interferon-a in newly diagnosed chronic myeloid leukemia. J Clin Oncol 2011;29:1634–42.

7. Nicolini F, Etienne G, Dubruille V, Roy L, Huguet F, Legros L, et al. Nilotinib and pegylated interferon alfa 2a for newly diagnosed chronic phase chronic myeloid leukaemia patients Results of a multicentric phase II study. Lancet Haematol 2015;2:e37-45.

8. Talpaz M, Hehlmann R, Quintás-Cardama A, Mercer J, and J Cortes. Re-emergence of interferon-α in the treatment of chronic myeloid leukemia. Leukemia 2013;27:803-12.

9. Essers MAG, Offner S, Blanco-Bose WE, Waibler Z, Kalinke U, Duchosal MA, et al. IFNα activates dormant haematopoietic stem cells in vivo. Nature 2009;458:904-909.

10. Sato T, Onai N, Yoshihara H, Arai F, Suda T, and T Ohteki. Interferon regulatory factor-2 protects quiescent hematopoietic stem cells from type I interferon-dependent exhaustion. Nature Med 2009;15(6):696-700.

11. Mahon FX, Rea D, Guilhot J, Guilhot F, Huguet F, Nicolini F, et al. Discontinuation of imatinib in patients with chronic myeloid leukaemia who have maintained complete molecular remission for at least 2 years: the prospective, multicentre Stop Imatinib (STIM) trial. Lancet Oncol 2010;11(11):1029-35.

12. Chomel, J-C, Bonnet M-L, Sorel N, Bertrand A, Meunier M-C, Fichelson S, et al. Leukemic stem cell persistence in chronic myeloid leukemia patients with sustained undetectable molecular residual disease Blood 2011;118(13):3657-60.

13. Beillard E, Pallisgaard N, van der Velden VH, Bi W, Dee R, van der Schoot E, et al. Evaluation of candidate control genes for diagnosis and residual disease detection in leukemic patients using 'real-time' quantitative reverse-transcriptase polymerase chain reaction (RQ-PCR) - a Europe against cancer program. Leukemia 2003;17(12):2474-86.

14. Cross NC, White HE, Müller MC, Saglio G, and A Hochhaus. Standardized definitions of molecular response in chronic myeloid leukemia Leukemia 2012;26(10):2172-5.

15. Kim P, Lee P, and D Levy. Dynamics and Potential Impact of the Immune Response to Chronic Myelogenous Leukemia. PloS Comp Biol 2008;4(6):e1000095.

16. Kantarjian HM, Giles F, Quintas-Cardama A, and J Cortes. Important therapeutic targets in chronic myelogenous leukemia. Clin Cancer Res 2007;13:1089–97.

17. Deininger M, Buchdunger E, and BJ Druker. The development of imatinib as a therapeutic agent for chronic myeloid leukemia. Blood 2005;105(7):2640-53.

18. Michor F, Hughes F, Iwasa Y, Branford S, Shah N, Sawyers C, et al. Dynamics of chronic myeloid leukaemia. Nature 2005;435(30):1267-1270.

19. Roeder I, Horn M, Glauche I, Hochhaus A, Mueller M, and M Loeffler. Dynamic modeling of imatinib-treated chronic myeloid leukemia: Functional insights and clinical implications. Nature Med 2006;12(10):1181-4.

20. Tang M, Gonen M, Quintas-Cardama A, Cortes J, Kantarjian H, Field C, et al. Dynamics of chronic myeloid leukemia response to long-term targeted therapy reveal treatment effects on leukemic stem cells. Blood 2011;118(6):1622-31.

21. Colijn C and M Mackey. A mathematical model of hematopoiesis -- I Periodic chronic myelogenous leukemia J Theoret Biol 2005;237:117-32.

22. Komarova N, and D Wodarz. Effect of Cellular Quiescence on the Success of Targeted CML Therapy. PLoS ONE 2007;10:e990.

23. Komarova N, Katouli AA, and D Wodarz. Combination of two but no three current targeted drugs can improve therapy of chronic myeloid leukemia. PLoS ONE 2009;4(2):e4423.

24. Marciniak-Czochra A, Stiehl T, Ho AD, Jäger W, and W Wagner. Modeling of asymmetric cell division in hematopoietic stem cells -- Regulation of self renewal is essential for efficient repopulation. Stem Cells and Development 2009;18:377-85.

25. Clapp G and D Levy. A Review of Mathematical Models for Treating Leukemia and Lymphoma Drug Discovery Today: Disease Models 2015: In press.

26. Burchert, A, Müller, MC, Kostrewa, P, Erben, P, Bostel, T, Liebler, S, et al. Sustained molecular response with interferon alfa maintenance after induction therapy with imatinib plus interferon alfa in patients with chronic myeloid leukemia. J Clin Oncol 2010;28:1429–35.

27. Burchert, A. Chronic myeloid leukemia stem cell biology and interferon alpha. Hematology Education 2014;8:87-96.

28. Laperrousaz B, Jeanpierre S, Sagorny K, Voeltzel T, Ramas S, Kaniewski B, et al. Primitive CML cell expansion relies on abnormal levels of BMPs provided by the niche and BMPRIb overexpression. Blood 2013;122(23):3767-77.

29. Mendelson A and PS Frenette. Hematopoietic stem cell niche maintenance during homeostasis and regeneration. Nature Medicine 2014;20(8):833-46.

30. Marin D, Bazeos A, Mahon F-X, Eliasson L, Milojkovic D, Bua M, et al. Adherence is the critical factor for achieving molecular responses in patients with chronic myeloid leukemia who achieve complete cytogenetic responses on imatinib. J Clin Onc 2010;28(14):2381-8.

31. DeConde R, Kim PS, Levy D, and PP Lee. Post-transplantation dynamics of the immune response to chronic myelogenous leukemia. J Theor Biol 2005;236:39-59.

32. Rufer N, Brummendorf T, Kolvraa S, Bischoff C, Christensen K, Wadsworth L, et al. Telomere fluorescence measurements in granulocytes and T lymphocyte subsets point to a high turnover of hematopoietic stem cells and memory T cells in early childhood. J Exp Med 1999;190(2), 157-67.

33. Mahmud N, Devine S, Weller K, Parmar S, Sturgeon C, Nelson M, et al. The relative quiescence of hematopoietic stem cells in nonhuman primates. Blood 2001;97:3061-8.

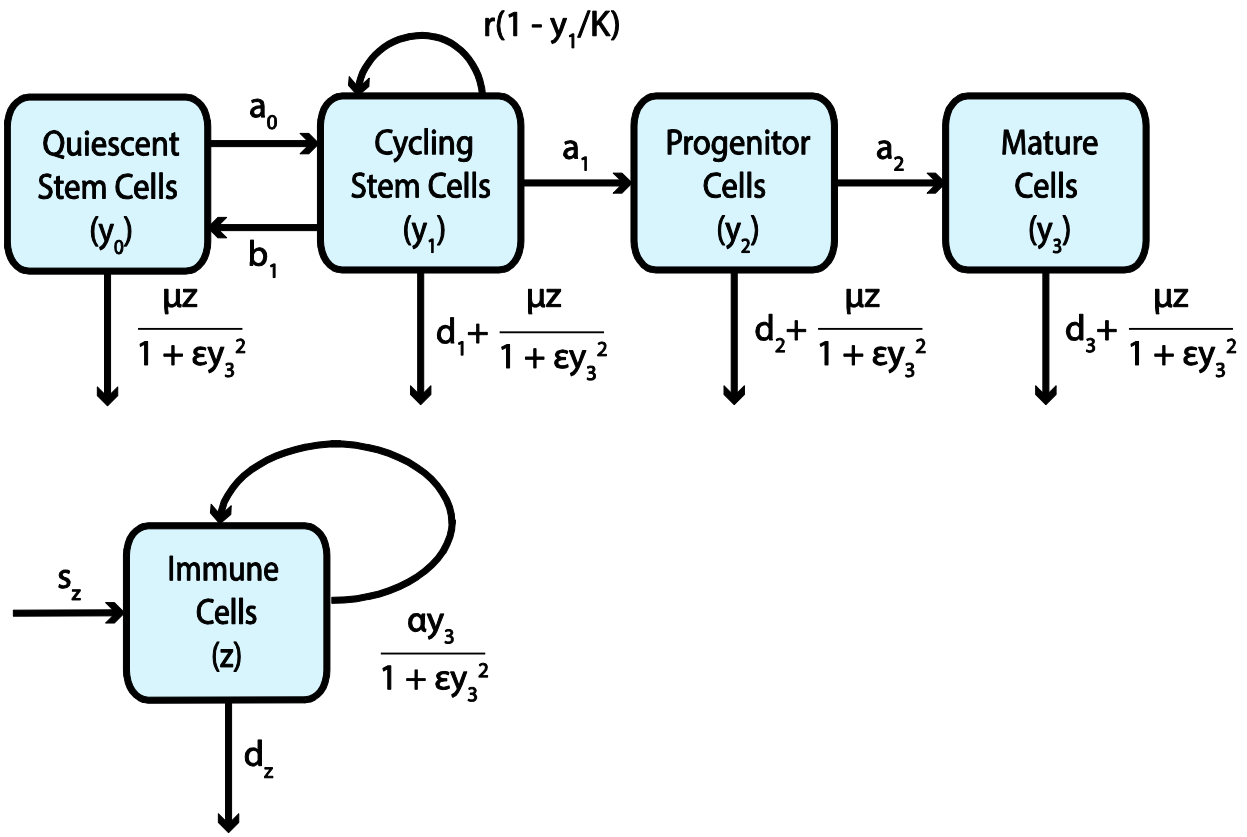

Figure 1. **Mathematical model including the intervention of the autologous immune system.**

In our model of CML and the immune response, we divide leukemic cells into quiescent stem cells (y_0), cycling stem cells (y_1), and progenitors (y_2), and mature cells (y_3). Stem cells transition between quiescence and cycling, and some cycling stem cells differentiate into progenitors cells, which can further differentiate into mature cells. Leukemic cells can die naturally at rates d_i or as a result of an interaction with immune cells (z). Immune cells are supposed in this disease to be supplied at a constant rate s_z and to die at a rate d_z. They can also be stimulated by leukemic cells to divide to produce more immune cells. Large leukemic populations are able to suppress the autologous immune system, by limiting immune cell expansion and limiting immune effector cells' ability to kill cancer cells.

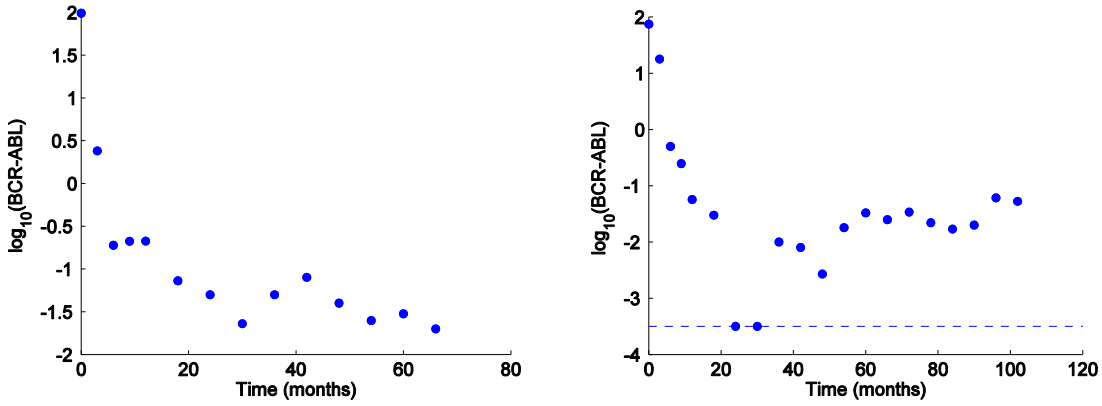

Figure 2. **Oscillations of the BCR-ABL ratio in two representative patients.**

During TKI therapy, a patient's progress is monitored by measuring their BCR-ABL ratio, which is a ratio of BCR-ABL mRNA expression to the expression of a control gene, in this case ABL. Both patients shown above were treated with standard IM 400 mg daily. During treatment, both patients show multiple increases in BCR-ABL ratio without overt relapse. Here, dots represent clinical data, and the dashed line approximates the detection threshold, or the lowest detectable leukemia level. Dots along this line mark indicate times measurements of zero, meaning the leukemia was undetectable within the limits of the assay. These figures correspond to patients 4 and 12 in Table S2 of the Supplementary Material.

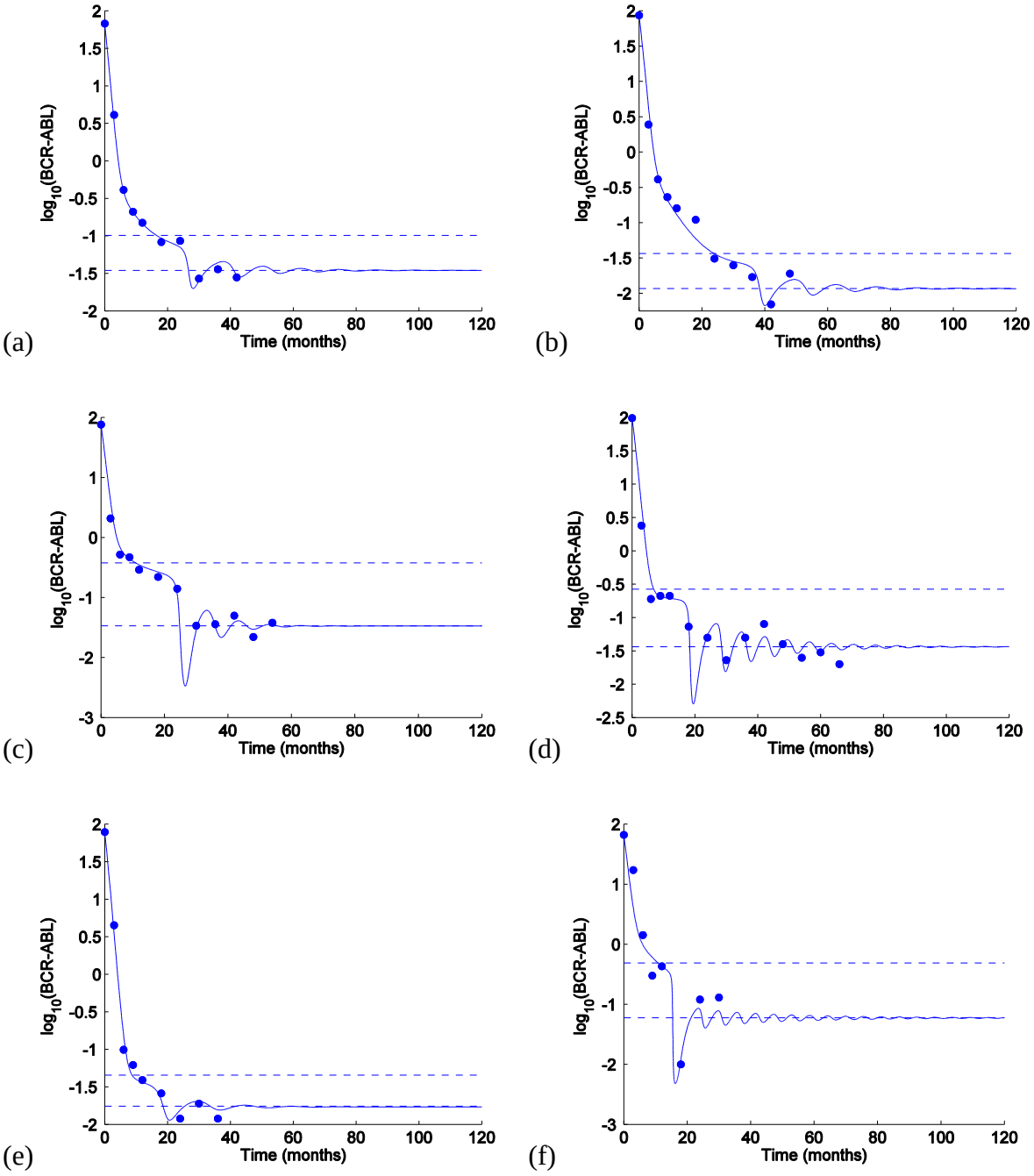

Figure 3. **Fits of our mathematical model to six representative patients.**

The base-10 log of the BCR-ABL ratio is plotted against time, in months. The dots represent patient data, and the solid lines represent our simulations. Dashed lines show the BCR-ABL ratios that correspond to the ends of immune window, y_{min} and y_{max}. These figures correspond to patients 1-6 in Table S2 of the Supplementary Material.

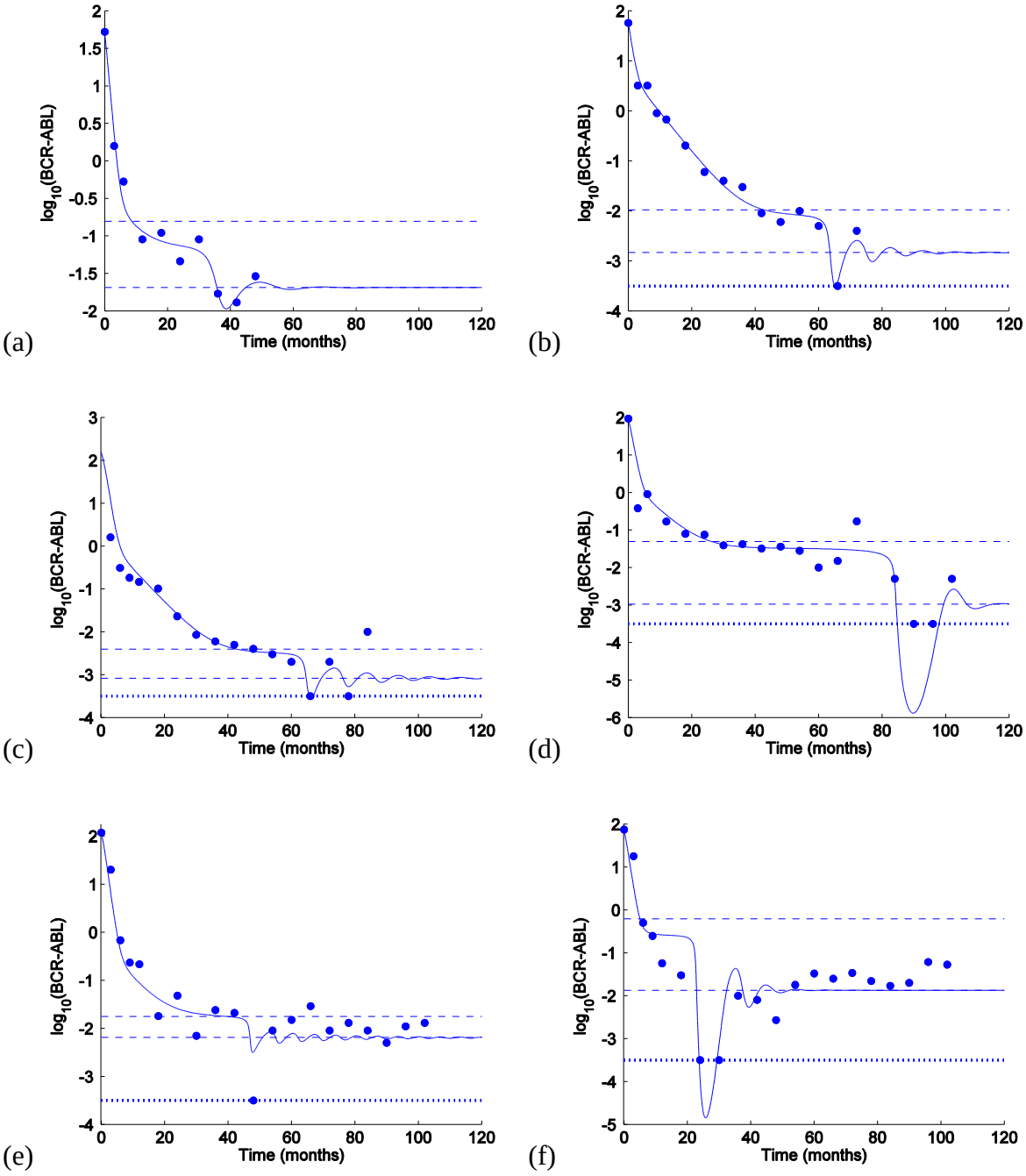

Figure 4. **Fits of our model to six additional patients.**

The base-10 log of the BCR-ABL ratio is plotted against time, in months. As in Figure 3, the dots represent patient data, and the solid lines represent our simulations. Dashed lines show the BCR-ABL ratios that correspond to the ends of immune window, y_{min} and y_{max}. Dotted lines approximate the minimum leukemic level that is detectable by RQ-PCR. Dots along this line represent zero measurements,

meaning CML cells were not detected. These figures correspond to patients 7-12 in Table S2 of the Supplementary Material.

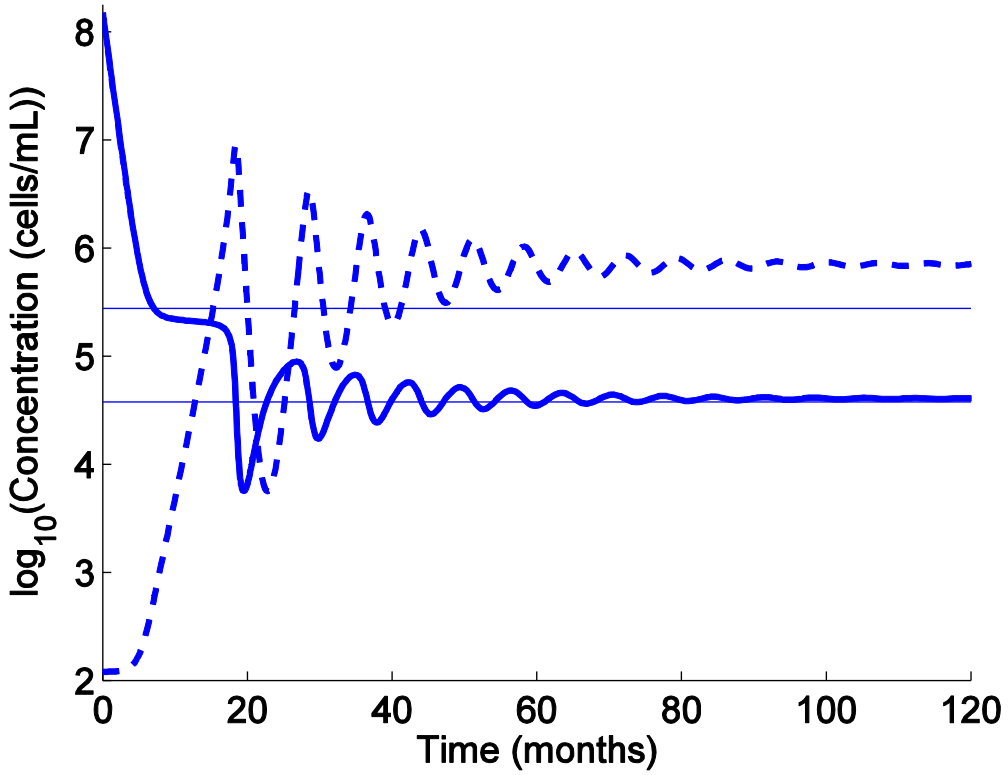

Figure 5. **Model simulation for a single representative patient.**

The base-10 log of the leukemia and immune cell populations, in cells/mL, are plotted as a function of time, in months. The thick solid line represents the total leukemic population ($y_0 + y_1 + y_2 + y_3$), and the thick dashed line represents the immune cell population (z). The thin solid lines show the immune window $[y_{min}, y_{max}] = [10^{4.58}, 10^{5.44}]$ cells/mL. For the first twenty months, the patient's leukemia load decreases monotonically, while the immune cells begin to expand. The leukemic population enters the immune window at around month 7. The immune cells mount an attack starting around month 18. This first attack results in the minimum leukemia load achieved during therapy, at around 10^4 cells/mL. The immune cells drive the leukemia load below the immune window, allowing the leukemic population to partially recover. The two populations oscillate with decreasing amplitudes as they approach their equilibrium concentrations of (y, z) = ($10^{4.61}$, $10^{5.85}$) cells/mL. This simulation corresponds to the plot in Figure 3d (patient 4 in Table S2).

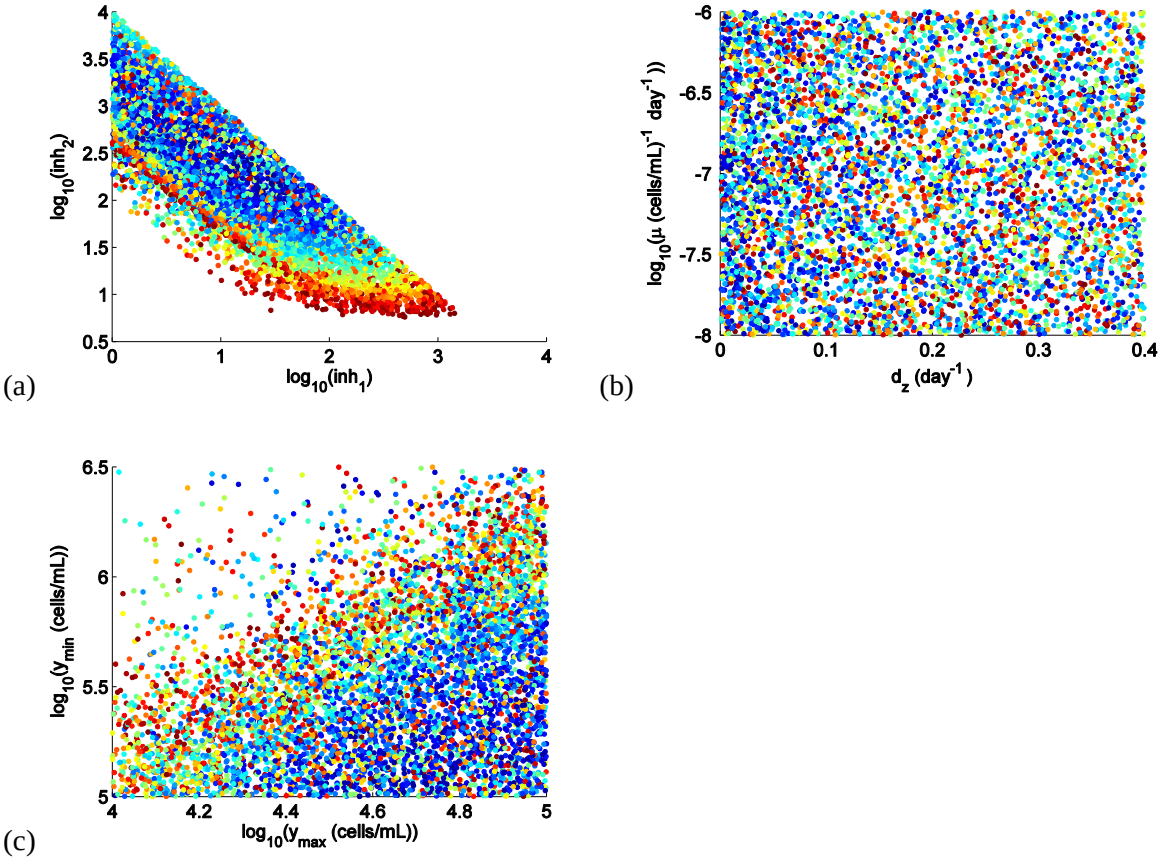

Figure 6. **Quality of the fit as a function of a pair of parameters, for a single representative patient.** This is the same patient whose simulation is shown in Figures 3d and 5 (patient 4 in Table S2). Red dots indicate worse fits, and dark blue dots indicate better fits. Here, we only show simulations that resulted in a total cost of less than 10, where cost is the squared log-distance between the patient data and model simulation. (a) $\log(inh_2)$ vs. $\log(inh_1)$. For this patient inhibition values satisfying $\log(inh_1\ inh_2)$ in [2, 4] were tested. These two parameters are strongly related to the quality of the fit. (b) $\log(\mu)$ vs. d_z. These two parameters seem to be the least important, as it is difficult to see any correlation between the fit and either of these parameters. (c) y_{max} vs. y_{min}. There is a definite relationship between the fit and these two variables. The worse fits tend to be in the upper left corner, while the better fits tend to be in the lower right corner. The parameters y_{max} and y_{min} determine the immune window and therefore affect the timing and magnitude of the autologous immune response.

Parameter	**log(inh_1)**	**log(inh_2)**	**d_T**	**log(μ)**	**log(y_{min})**	**log(y_{max})**	**log(y_{max} / y_{min})**
Mean	1.132	2.487	0.099	-7.047	3.970	5.024	1.053
STD	0.830	0.754	0.097	0.636	0.888	0.804	0.499
Max	2.772	3.880	0.371	-5.896	5.483	6.024	2.006
Min	0.024	1.073	0.005	-7.954	2.548	3.226	0.197

Table 1. **Summary of parameter values used in our model simulations.**

Of the 65 patients IM patients who do not relapse, develop drug resistance, or progress, 22 change their IM dose during therapy. An additional 6 patients have non-IS measurements, and 11 patients have five or fewer measurements. We focus on the remaining 25 patients and present the mean, standard deviation, maximum, and minimum parameter values.

Supplementary Material

Parameter	Description	Value	Source
$y_0(0)$	Initial leukemic quiescent stem cell concentration	37.5000	Estimated based on [18]
$y_1(0)$	Initial leukemic cycling stem cell concentration	4.1667	Estimated based on [18]
$y_2(0)$	Initial leukemic progenitor concentration	$1.6667(10)^4$	[18]
$y_3(0)$	Initial leukemic mature cell concentration	$1.5(10)^8$	[31]
$z(0)$	Initial autologous immune cell concentration	120	Estimated based on [31]
a_0	Stem cell transition rate to cycling	0.0027	Estimated
b_1	Stem cell transition rate to quiescence	0.0247	Estimated
r	Cycling stem cell growth rate	0.08	Estimated based on [15]
K	Cycling stem cell carrying capacity	4.2872	Estimated
a_1	Differentiation rate and expansion factor for progenitors	24.0005	Estimated
a_2	Differentiation rate and expansion factor for mature cells	899.9820	Estimated
d_1	Cycling stem cell death rate	0.00225	[15]
d_2	Progenitor cell death rate	0.006	[15]

d_3	Mature cell death rate	0.0375	[15]
s_z	Source term for autologous immune cells	$120 * d_z$	Estimated
β	Adjustment factor for BCR-ABL ratio	3	Estimated based on patient data

Table S1. Universal parameter estimates. This table provides the values of the universal parameters. Cell concentrations are in cells/mL. The initial values $y_0(0) + y_1(0)$ and $y_2(0)$ are chosen based on the initial number of leukemic stem $(2.5(10)^5$ cells) and precursor cells $(1(10)^8$ cells) in [18], converted to cells/mL by assuming a blood volume of 6 L. The value $y_3(0)$ is estimated in [31]. The value $z(0)$ is also based on [31], assuming a concentration of $6(10)^5$ cells/mL, of which about 1/5000 is specific to leukemia. Quiescent stem cells enter the cell cycle infrequently [32], so we set a_0 equal to 1/365 days^{-1}. The parameter b_1 is set to $9a_0$ so that most stem cells in our model are quiescent, which is in agreement with [33]. Thus, the two stem cell populations will approximately have a 1:9 ratio, so we set $y_0(0) = 0.1\ (y_0(0) + y_1(0))$ and $y_1(0) = 0.1\ (y_0(0) + y_1(0))$. The death rates d_1, d_2, and d_3 are set to those in [15]. The stem cell growth rate is also based on the value in [15]. We increase the original value ($r = 0.008$) by a factor of 10 to account for the fact that only 10% of the stem cells in our model contribute to growth, while all stem cells contribute to growth in [15]. The parameters K, a_1, and a_2 are selected so that the initial conditions represent a steady state when the immune response is removed from the model. (That is, $y_1(0) = K(r - d_1)/r$, $y_0(0) = b_1y_1(0)/a_0$, $y_2(0) = a_1y_1(0)/d_2$, and $y_3(0) = a_2y_2(0)/d_3$.) We assume that $z(0) = s_z / d_z$, so the value of d_z determines s_z. Lastly, the adjustment factor β is selected based on the maximum BCR-ABL ratio (269) in our data set.

Patient	inh_1	inh_2	d_T	μ	y_{min}	y_{max}
1	9.944	131.016	0,187	$4.021(10)^{-8}$	$6.001(10)^{4}$	$1.754(10)^{5}$
2	33.268	148.517	0.131	$1.515(10)^{-8}$	$1.443(10)^{4}$	$4.521(10)^{4}$
3	4.612	92.3215	0.031	$9.964(10)^{-7}$	$4.994(10)^{4}$	$5.598(10)^{5}$
4	1.456	545.150	0.099	$1.504(10)^{-8}$	$3.765(10)^{4}$	$2.759(10)^{5}$
5	1.872	1700.274	0.128	$3.082(10)^{-7}$	$2.482(10)^{4}$	$6.513(10)^{4}$
6	9.652	43.752	0.238	$1.350(10)^{-7}$	$1.050(10)^{5}$	$8.637(10)^{5}$
7	5.771	155.963	0.019	$4.057(10)^{-8}$	$4.846(10)^{4}$	$3.695(10)^{5}$
8	591.591	14.568	0.040	$2.371(10)^{-7}$	$3.132(10)^{3}$	$2.228(10)^{4}$
9	486.315	226.000	0.075	$2.879(10)^{-8}$	$3.536(10)^{2}$	$1.684(10)^{3}$
10	50.988	79.645	0.005	$1.271(10)^{-6}$	$1.182(10)^{3}$	$5.482(10)^{4}$
11	30.208	359.979	0.371	$2.263(10)^{-7}$	$4.959(10)^{3}$	$1.353(10)^{4}$
12	1.5201	265.6435	0.015	$2.748(10)^{-8}$	$2.031(10)^{4}$	$9.352(10)^{5}$

Table S2. Patient-specific parameter estimates.

Parameter values for patients 1-6 were used to produce Figure 3, while parameter values for patients 7-12 were used to produce Figure 4. Here, y_{min} and y_{max} can be used to obtain immune parameters $\varepsilon = 1 / (y_{min}\, y_{max})$ and $\alpha = (y_{min}\, y_{max})\, \varepsilon d_z$.